



| | |
|------------------|--|
| Title | Correlation between some physical properties of titanium dioxide particles and their photocatalytic activity for some probe reactions in aqueous systems |
| Author(s) | Kominami, Hiroshi; Murakami, Shinya; Kato, Junichi; Kera, Yoshiya; Ohtani, bunsho |
| Citation | Journal of physical chemistry. B, 106(40), 10501-10507 https://doi.org/10.1021/jp0147224 |
| Issue Date | 2002-10-10 |
| Doc URL | http://hdl.handle.net/2115/52788 |
| Type | article |
| File Information | jp0147224.pdf |



[Instructions for use](#)

Correlation between Some Physical Properties of Titanium Dioxide Particles and Their Photocatalytic Activity for Some Probe Reactions in Aqueous Systems

Hiroshi Kominami,^{*,†,‡} Shin-ya Murakami,[†] Jun-ichi Kato,[†] Yoshiya Kera,^{†,‡} and Bunsho Ohtani[§]

Department of Applied Chemistry, Faculty of Science and Engineering, Kinki University, Kowakae, Higashiosaka, Osaka 577-8502, Japan, Open Research Center, Kinki University, Kowakae, Higashiosaka, Osaka 577-8502, Japan, and Catalysis Research Center, Hokkaido University, Sapporo 060-0811, Japan

Received: December 31, 2001; In Final Form: July 29, 2002

Nanocrystalline anatase titanium(IV) oxide (TiO₂) particles were synthesized by hydrothermal crystallization in organic media (HyCOM) followed by calcination at various temperatures up to 1273 K, and they were characterized by analysis of surface adsorption of the substrates, as well as by X-ray diffraction (XRD) and Brunauer–Emmet–Teller (BET) surface area measurements. These HyCOM TiO₂ samples were used for three kinds of photocatalytic reactions: mineralization of acetic acid (AcOH) in aerated aqueous suspensions, dehydrogenation of 2-propanol (2-PrOH) by in situ platinized powders, and silver-metal deposition from silver ions (Ag⁺) in deaerated aqueous suspensions of bare TiO₂ samples. Dependence of the photocatalytic activities on calcination temperature (*T_c*) and on the amount of adsorbed substrates in each reaction and correlations with the physical properties of HyCOM TiO₂ were examined. In the case of mineralization of AcOH, the activity of each sample was almost proportional to the amount of surface-adsorbed AcOH in the dark, and the uncalcined (as-prepared) HyCOM TiO₂ showed the highest activity, which was monotonically reduced with *T_c*, that is, with decrease in the amount of surface-adsorbed AcOH. On the other hand, in the case of silver-metal deposition, the photocatalytic activity was enhanced by calcination at higher temperature, despite the simultaneous decrease in the amount of surface-adsorbed Ag⁺ in the dark. Overall, the effects of calcination on the photocatalytic activities for several reaction systems strongly suggested that photocatalytic activity depends on two significant factors, adsorbability and recombination probability, corresponding to the specific surface area and crystallinity, respectively, and that the balance of these two factors determines the *T_c* dependence.

I. Introduction

Semiconductor photocatalytic reactions, such as water splitting,^{1–8} dehydrogenation of alcohols,^{9–13} mineralization of organic compounds in water,^{14–17} organic syntheses,^{18–22} and reductive fixation of carbon dioxide,^{23–29} are of great importance for both fundamental studies and practical applications. Among the various semiconductor photocatalysts, titanium(IV) oxide (TiO₂) is one of the most popular and promising materials because it is stable in various solvents under photoirradiation, it is available commercially, and it can induce various types of redox reactions.^{30,31} High efficiency of utilization of adsorbed light energy, that is, enhancement of photocatalytic activity, is needed for applications of photocatalytic reactions. It has been reported that the photocatalytic activity of TiO₂ powder differs depending on the preparation and treatment conditions. Various factors that affect the photocatalytic activity have been reported, including crystal structure (anatase or rutile),^{32–34} particle size,^{35–38} surface area,³⁹ and surface hydroxyls.^{40–42} In most studies, attempts were made to correlate the photocatalytic activity in only one reaction system examined with only one physical property of the photocatalysts. Moreover, the variation of physical properties of TiO₂ was limited. The TiO₂ samples

used so far have been prepared by hydrolysis of titanium compounds and dehydration,^{43,44} sol–gel,⁴⁵ a hydrothermal method,^{46,47} or modification of commercially available TiO₂. Generally speaking, it is difficult to control the physical properties of TiO₂ samples precisely and independently because the properties are related to each other and they are modified simultaneously; for example, the specific surface area is determined by the particle size and its distribution. Therefore, care is needed in drawing calculations on the decisive factor of activity in each photocatalytic reaction system and in rationalizing the correlation by clarifying the kinetics.

In a series of studies on TiO₂ photocatalytic reactions,^{48–53} we have shown that the overall kinetics depends on both the rates of reduction and oxidation by a photoexcited electron (e⁻) or positive hole (h⁺), respectively, and the rate of recombination of e⁻ and h⁺. To obtain a highly active TiO₂ photocatalyst, therefore, it is necessary to synthesize a TiO₂ powder that has contradictory properties, that is, large surface area to adsorb substrates and high crystallinity (or lesser surface and bulk defects) to diminish the e⁻–h⁺ recombination. We have shown that nanocrystalline anatase TiO₂ having both high crystallinity and large surface area could be synthesized by high-temperature hydrolysis of titanium alkoxides with a limited amount of water dissolved in organic solvents and concomitant crystallization (HyCOM; *hydrothermal crystallization in organic media*).^{54,55} The HyCOM TiO₂ powders exhibited activities a few times higher than those of Degussa P-25 TiO₂ for photocatalytic

* To whom correspondence should be addressed. E-mail: hiro@apch.kindai.ac.jp.

[†] Department of Applied Chemistry, Faculty of Science and Engineering, Kinki University.

[‡] Open Research Center, Kinki University.

[§] Catalysis Research Center, Hokkaido University.

reactions under deaerated conditions such as dehydrogenation of 2-propanol (2-PrOH),⁵⁶ silver-metal (Ag) deposition,^{56,57} and N-cyclization of (*s*)-lysine,⁵⁸ as well as mineralization of acetic acid (AcOH)⁵⁹ in aqueous solutions under aerated conditions. The above hypothesis has been supported by the ultrahighly active TiO₂ photocatalyst synthesized by this newly developed HyCOM method. HyCOM TiO₂ shows high thermal stability and possesses a large surface area even after calcination at 973 K, indicating that the physical properties of HyCOM TiO₂ powders can be systematically controlled over a wide range by changing calcination temperature, *T_c*.⁵⁷

We have precisely measured the amount of silver ions (Ag⁺) adsorbed on the surfaces of HyCOM TiO₂ samples in the dark under conditions similar to the photocatalytic reaction and have reported preliminary results showing correlations of the physical properties (adsorbability and recombination probability) with photocatalytic activities of HyCOM TiO₂ for silver-metal (Ag) deposition.⁵⁷ In this study, a series of HyCOM TiO₂ samples with various physical properties were prepared by changing *T_c*, and they were used for three photocatalytic reactions, that is, photocatalytic oxidative decomposition, mineralization of AcOH in aqueous aerated solutions,^{16,59–61}



dehydrogenation of 2-PrOH in deaerated aqueous solutions, and oxygen (O₂) liberation along with Ag deposition from deaerated Ag₂SO₄ solutions. Here, we show the detailed characterization of these reactions and discuss the correlation of photocatalytic activities of HyCOM TiO₂ with the physical properties, especially adsorbability and recombination probability, for design of highly active TiO₂ photocatalysts.

II. Experimental Section

Sample Preparation. HyCOM TiO₂ powders were synthesized by a procedure reported previously;^{54,55} titanium(IV) butoxide (25 g) in toluene (70 cm³) was heated at 573 K for 2 h in an autoclave in the presence of water (10 or 25 cm³) fed in a space separated from the alkoxide solution. The resulting powders were washed repeatedly with acetone and dried in air at ambient temperature. The TiO₂ powders obtained by this method in the presence of 10 and 25 cm³ of water are called HyCOM-A and HyCOM-B, respectively. As-prepared HyCOM-A and HyCOM-B were calcined in a box furnace at various temperatures under a flow of air (30 cm³ min⁻¹); the sample in a combustion boat was heated to the desired temperature at a rate of 10 K min⁻¹, held at that temperature for 1 h, and then cooled to room temperature. The thus-calcined sample is designated HyCOM-A (or HyCOM-B) (calcination temperature); for example, HyCOM-A(973) means a HyCOM-A sample calcined at 973 K. Platinization (0.1 wt %) of TiO₂ (50 mg) was performed by the photochemical deposition method from an aqueous solution (5 cm³) of tetraammineplatinum(II) chloride ([Pt(NH₃)₄]Cl₂, Wako Pure Chemical, 4.56 mg Pt cm³) under irradiation with a 400-W high-pressure mercury arc (Eikousha) at 298 K with vigorous magnetic stirring (1000 rpm). Pretreatment was carried out to decompose contaminated organic moieties on the TiO₂ surface; TiO₂ powder (50 mg) was suspended in 5 cm³ of water in a glass test tube and photoirradiated at $\lambda > 300$ nm by a high-pressure mercury arc (400 W) under oxygen with magnetic stirring until carbon dioxide was no longer liberated. Degussa P-25 TiO₂ was used as a reference in most of the experiments because it is known to be one of the most active photocatalysts.

Characterization of HyCOM TiO₂ Powders. Powder X-ray diffraction (XRD) of Cu K α radiation was measured using a Rigaku RINT 2500 equipped with a carbon monochromator. Crystallite size (*d*₁₀₁) of anatase was calculated from the Scherrer equation and half-height width of the 101 diffraction peak of anatase. The specific surface area (*S*_{BET}) was calculated by the Brunauer–Emmet–Teller (BET) single-point method on the basis of nitrogen (N₂) uptake measured at 77 K at the relative pressure of 0.3. Before the N₂ adsorption, each sample was dried at 423 K for 15 min in a 30% N₂–helium flow.

Photoirradiation and Product Analyses. (A) For photocatalytic reaction in an aqueous AcOH solution, bare TiO₂ powder (50 mg) was suspended in an AcOH solution (0.2–35 mmol dm⁻³, 5.0 cm³). (B) For photocatalytic reaction in an aqueous silver sulfate (Ag₂SO₄) solution, bare TiO₂ powder (50 mg) was suspended in a Ag₂SO₄ solution (0.5–25 mmol dm⁻³, 5.0 cm³). (C) For photocatalytic reaction in an aqueous 2-PrOH solution, Pt (0.1 wt %)-TiO₂ powder (50 mg) was suspended in a 2-PrOH solution (0.50 mmol, 5.0 cm³). (D) For photocatalytic reaction in an aqueous Ag₂SO₄–2-PrOH solution, bare TiO₂ powder (50 mg) was suspended in an aqueous solution of Ag₂SO₄ (25 mmol dm⁻³, 5.0 cm³) containing 2-PrOH (0.50 mmol). The reactions of A and B were carried out in reaction tubes (18 mm in diameter and 180 mm in length, transparent for light with a wavelength of >300 nm) under aerated conditions, while those of C and D were carried out under an Ar atmosphere. The suspension was stirred (1000 rpm) at 298 K by using a magnet bar. After the irradiation, the amounts of carbon dioxide (CO₂) and hydrogen (H₂) in the gas phase of reaction mixtures were measured using a Shimadzu GC-8A gas chromatograph equipped with Porapak QS (CO₂) and MS-5A (O₂ and H₂) columns. The amounts of 2-PrOH and acetone were analyzed using a Shimadzu GC-8A gas chromatograph equipped with an FID and a column packed with PEG20M. Deposited Ag was analyzed by inductively coupled plasma emission spectroscopy (ICP, Shimadzu ICPS-1000III) after dissolution with concentrated nitric acid (HNO₃).

Adsorption Measurements. TiO₂ was added to the AcOH and Ag⁺ solutions in the dark under conditions similar to those of the photocatalytic reactions. Then the TiO₂ was separated by centrifugation. The amounts of AcOH and Ag⁺ adsorbed on the surface of TiO₂, *C*_{ads}(AcOH) and *C*_{ads}(Ag⁺), were determined from the difference between concentrations before and after the addition of TiO₂ by titration with an aqueous sodium hydroxide (NaOH) solution and by ICP, respectively.

III. Results and Discussion

Physical Properties of As-Prepared and Calcined HyCOM-TiO₂ Powders. The physical properties of HyCOM-A and -B are summarized in Table 1. Both of the as-prepared HyCOM-A and -B (HyCOM-A(unc) and B(unc)) powders consisted of nanosized crystallites (11 and 12 nm, respectively) with relatively large surface areas (>120 m² g⁻¹). We have reported that HyCOM-B(unc) consisted of the agglomerates of primary particles of an average diameter of 12.6 nm on the basis of transmission electron microscopic investigations.⁵⁵ The diameter was shown to be in good agreement with the crystallite size calculated from the Scherrer equation, indicating that HyCOM samples are composed of single crystals in nanosize. With calcination, the surface area gradually decreased with increasing *T_c*, showing growth of crystallites. This dependence on *T_c* has often been observed when TiO₂ samples are calcined at different temperatures.¹³ However, it should be noted that even after calcination at 973 K, the anatase phase in HyCOM-A

TABLE 1: Physical Properties of As-prepared and Calcined HyCOM-A and -B

| TiO ₂ | T _c (K) ^a | crystallite ^b | d ₁₀₁ (nm) ^c | S _{BET} (m ² g ⁻¹) ^d |
|------------------|---------------------------------|--------------------------|------------------------------------|---|
| HyCOM-A | | A | 11 | 140 |
| HyCOM-A | 573 | A | | 133 |
| HyCOM-A | 823 | A | 18 | 78 |
| HyCOM-A | 923 | A | | 38 |
| HyCOM-A | 973 | A | 26 | 21 |
| HyCOM-A | 1073 | A, R | 47 | 8 |
| HyCOM-A | 1173 | A, R | 55 | 5 |
| HyCOM-A | 1273 | A, R | | 3 |
| HyCOM-B | | A | 12 | 123 |
| HyCOM-B | 823 | A | 15 | 93 |
| HyCOM-B | 973 | A | 21 | 69 |
| HyCOM-B | 1073 | A | 25 | 58 |
| HyCOM-B | 1173 | A, R | 57 | 17 |
| P-25 | | A, R | 25 | 50 |

^a HyCOM-A and B powders were prepared at 573 K in toluene and calcined at T_c. ^b A = anatase; R = rutile. ^c Crystallite size calculated from the 101 diffraction peak of the anatase phase. ^d BET surface area.

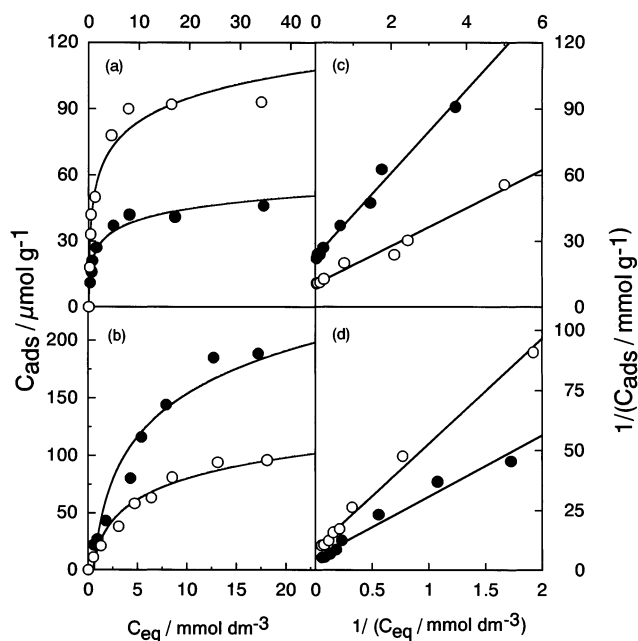


Figure 1. Isotherms of adsorption of (a) AcOH and (b) Ag⁺ and (c, d) their double reciprocal plots fitting to the Langmuir equation. Closed circles show data of P-25, and open circles show data of (a, c) HyCOM-B(unc) or (b, d) HyCOM-A(973).

remained and the sample had a large surface area of 21 m² g⁻¹. Furthermore, an increase in the amount of water fed into the autoclave resulted in an increase in crystallinity and in thermal stability of TiO₂; a rutile phase was not observed even in HyCOM-B(1073) as shown in Table 1. The effects of preparation conditions on the physical properties have been discussed in detail elsewhere.⁵⁵

Mineralization of an Acetic Acid System. Figure 1a shows the amounts of AcOH adsorption on HyCOM-B(unc) and P-25 as a function of equilibrium concentration of AcOH (C_{eq}(AcOH)). Both TiO₂ samples gave Langmuirian isotherms. From the linear double-reciprocal plots (Figure 1c), the adsorption equilibrium constant (K_{ads}(AcOH)) and limiting amount of C_{ads}(AcOH) (C_{ads}^{max}(AcOH)) were estimated and are shown in Table 2, together with density of adsorbed molecules in a unit area of the TiO₂ surface (d_{ads}). K_{ads} and d_{ads} of HyCOM-B(unc) were almost the same as those of P-25, suggesting a similar nature of adsorption of AcOH on their surfaces; the relatively larger adsorption on the HyCOM-B(unc) surface is attributed to its

larger specific surface area. A similar tendency could be seen for Ag⁺ adsorption, as is discussed later.

A time course profile of photocatalytic liberation of CO₂ by HyCOM-B(unc) is shown in Figure 2. As reported previously for different AcOH concentrations,⁵⁹ the yield of CO₂ linearly increased with photoirradiation time, just before complete consumption of AcOH, which shows zero-order kinetics for the reaction. The final yield of CO₂ coincided well with twice the molar amount of AcOH, indicating that complete mineralization of AcOH, according to eq 1, had occurred.

Figure 3a shows the rate of photocatalytic CO₂ formation (r(CO₂)) by each TiO₂ sample as a function of C_{ads}(AcOH). For HyCOM-B(unc), an almost linear relation was observed in the C_{ads} range below 0.050 mmol g⁻¹, and slight saturation of r was seen at the higher values of C_{ads}. Because HyCOM-B(unc) was actually ca. 2-fold more active than was P-25 when compared with the same concentration of AcOH, the similar relations between r and C_{ads} for both TiO₂ samples suggested that the photocatalytic activity in this reaction system is proportional to the specific surface area or, in other words, to the amount of reaction substrates. From the linear part of this plot, the following empirical formula for HyCOM-B(unc) for AcOH mineralization with a coefficient k(CO₂/AcOH-HyCOM-B(unc)) of 19.8 was obtained.

$$r (\mu\text{mol h}^{-1}) = k C_{\text{ads}} (\mu\text{mol g}^{-1}) \quad (2)$$

The adsorption of AcOH in the dark could not be same as that under irradiation. Actually photoadsorption of gaseous O₂ onto TiO₂ surfaces had been reported.⁶² However, the adsorption of AcOH in the dark should clearly indicate a trend in adsorption, that is, the latter should increase with the increase in the former. On the basis of the assumption that AcOH is converted directly to CO₂, the time-course curve was simulated and is shown in Figure 2. The observed zero-order kinetics is attributed to the saturated surface adsorption even at low C_{eq}(AcOH). Using the data of P-25 in Figure 3a, we estimated that the coefficient k(CO₂/AcOH-P-25) of the empirical rate expression (eq 2) was a little smaller than that for HyCOM-B(unc). As discussed later, the coefficient may be related to the intrinsic activity of TiO₂, that is, the e⁻-h⁺ recombination kinetics of each TiO₂ sample. In a previous paper,⁶³ we investigated the recombination kinetics after photoexcitation by femtosecond pump-probe diffuse reflectance spectroscopy and found that the second-order rate constant for e⁻-h⁺ recombination in HyCOM-B(unc) was 1.3–1.5 times smaller than that in P-25, which is consistent with the difference in the coefficients in this study.

Figure 3b shows r(CO₂) by the calcined HyCOM-B powders. Calcination at a higher temperature gave a smaller surface area, resulting in smaller C_{ads}(AcOH), which was almost proportional to their BET surface area (Figure 4a). This suggests similar d_{ads} and thereby that the adsorption characteristics of AcOH are not changed by calcination. Taking into account the slight saturation shown above (Figure 3a) for HyCOM-B(unc), we could not point out a linear relation between r(CO₂) and C_{ads}(AcOH), but it can be concluded that the photocatalytic activity in this reaction system was mainly determined by C_{ads}(AcOH). These results suggest that TiO₂ samples with large surface areas and thereby high adsorbability exhibit large r(CO₂). However, as we have shown previously,⁵⁹ amorphous TiO₂ (Idemitsu UF) without a crystalline phase gave negligible r(CO₂), though it had a large surface area (> 300 m² g⁻¹). These findings suggest that the minimal requisites for a photocatalyst of high activity are some degree of crystallinity and a large surface area.

TABLE 2: Langmuirian Parameters of TiO₂ Samples

| TiO ₂ | S_{BET} (m ² g ⁻¹) | AcOH | | | Ag ⁺ | | |
|------------------|---|---|---|--|---|---|--|
| | | K_{ads} (mol ⁻¹ dm ³) ^a | $C_{\text{ads}}^{\text{max}}$ (μmol g ⁻¹) ^b | d_{ads} (nm ⁻²) ^c | K_{ads} (mol ⁻¹ dm ³) ^a | $C_{\text{ads}}^{\text{max}}$ (μmol g ⁻¹) ^b | d_{ads} (nm ⁻²) ^c |
| HyCOM-B(unc) | 123 | 1187 | 97 | 0.48 | | | |
| HyCOM-A(973) | 34 | | | | 210 | 109 | 1.9 |
| P-25 | 50 | 1216 | 43 | 0.52 | 205 | 192 | 2.3 |

^a Adsorption equilibrium constant. ^b Limiting amount of substrates adsorbed on the surface of TiO₂. ^c Density of adsorbed substrates in a unit area of the TiO₂ surface.

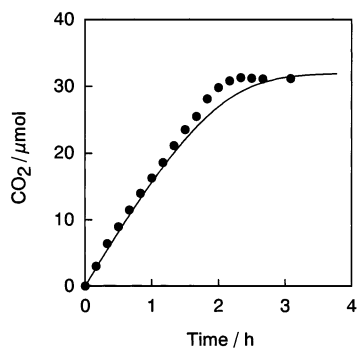


Figure 2. Time course of photocatalytic CO₂ liberation by HyCOM-B(unc) photocatalyst (50 mg) suspended in aqueous AcOH (16 μmol) solution (5.0 cm³). The 400 W high-pressure mercury arc was used. The solid line shows the results of simulation with the estimated constants shown in Table 2.

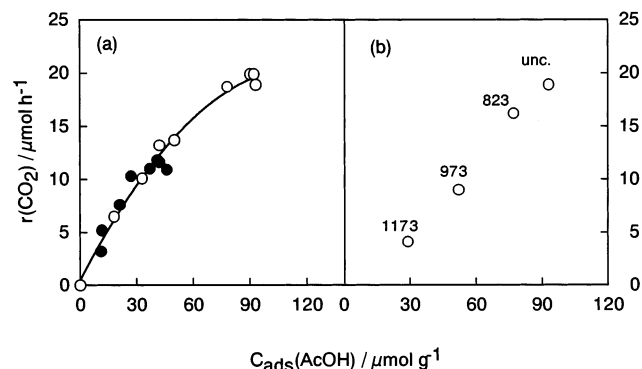


Figure 3. Rate of photocatalytic CO₂ liberation ($r(\text{CO}_2)$) as functions of the amounts of adsorbed AcOH ($C_{\text{ads}}(\text{AcOH})$) on (a) HyCOM-B(unc) (○) and P-25 (●) in the dark and (b) HyCOM-B(unc) and HyCOM-B samples calcined at T_c given in the figure.

The apparent T_c dependence of $r(\text{CO}_2)$ by HyCOM-B is shown in Figure 5a, as well as that by HyCOM-A (Figure 5a'). Because, in these $r(\text{CO}_2)$ measurements, different light sources (100- and 400-W high-pressure mercury arc lamps, respectively) were used, we could not compare the results directly, but it is clear that the T_c dependencies for both HyCOM samples are essentially the same, depending predominantly on $C_{\text{ads}}(\text{AcOH})$.

Ag Deposition–Oxygen Liberation System. As has been reported⁵⁷ and shown in Figure 1b, adsorption of Ag⁺ ($C_{\text{ads}}(\text{Ag}^+)$) on HyCOM-A(973) and P-25 TiO₂ powders obeys Langmuirian isotherms, similar to those of AcOH (Figure 1a). The constants were determined from the double-reciprocal plots in Figure 1d and are shown in Table 2. Again, HyCOM and P-25 gave almost the same values of K_{ads} and d_{ads} , suggesting a similar nature of Ag⁺-adsorption sites on the TiO₂ surfaces and similar densities (d_{ads}).

Photoirradiation of TiO₂ particles suspended in an aqueous Ag₂SO₄ solution led to the liberation of O₂ in the gas phase together with deposition of Ag on the TiO₂ surfaces. The molar ratios of these products were ca. 4, except for the cases of

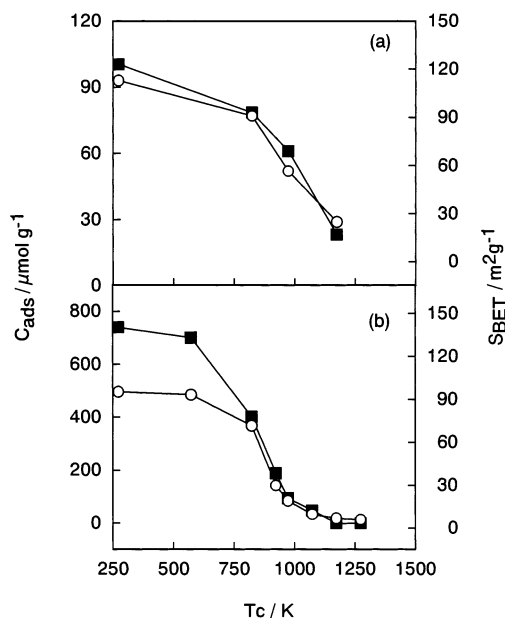
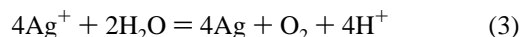


Figure 4. Dependence of the calcination temperature (T_c) on (○) the amount of adsorption of (a) AcOH and (b) Ag⁺ in the dark and (■) specific surface area of (a) HyCOM-B and (b) HyCOM-A.

smaller yields, satisfying the following stoichiometry:



It has been proved that pH decrease by the liberated proton causes protonation of surface hydroxyls resulting in inhibition of the adsorption of cations.^{41,50} To avoid the effect of change in $C_{\text{ads}}(\text{Ag}^+)$ during the photoirradiation, the rate of the photocatalytic reaction ($r(\text{Ag})$) was estimated from the yield of deposited Ag by a short irradiation time, for example, 5 min. By adjusting the Ag⁺ concentration, we examined the relation between $r(\text{Ag})$ and $C_{\text{ads}}(\text{Ag}^+)$, and we revealed reasonable linearity for both HyCOM-A(973) and P-25, as shown in Figure 6.⁵⁷ Such dependence of $r(\text{Ag})$ on $C_{\text{ads}}(\text{Ag}^+)$ was first reported, to the best of our knowledge, by Fleischauer and co-workers⁶⁴ and recently by Martin and co-workers.⁶⁵ The coefficients $k(r(\text{Ag})/C_{\text{ads}}(\text{Ag}^+)-\text{HyCOM-A(973)})$ and $k(r(\text{Ag})/C_{\text{ads}}(\text{Ag}^+)-\text{P-25})$ were estimated to be 1.3 and 0.45, respectively, from the slope of the $r(\text{Ag}^+)-C_{\text{ads}}(\text{Ag}^+)$ plot in Figure 6, presumably reflecting the recombination rate in the TiO₂ particles; the rate constant for e⁻-h⁺ recombination for HyCOM-A(973) was 2–2.5 times smaller than that for P-25,⁶³ which is almost consistent with the ratio of the coefficient k in this system. Thus, for each TiO₂, the rate of the photocatalytic reaction, that is, photocatalytic activity, is governed by the amount of surface-adsorbed substrate(s).

Figure 4b shows $C_{\text{ads}}(\text{Ag}^+)$ and S_{BET} of HyCOM-A(973) as functions of T_c . These changes resembled those observed for AcOH adsorption (Figure 4a). Because an almost constant density of Ag⁺ adsorption, $d_{\text{ads}}(\text{Ag}^+)$, of ca. 2.5 nm⁻² was

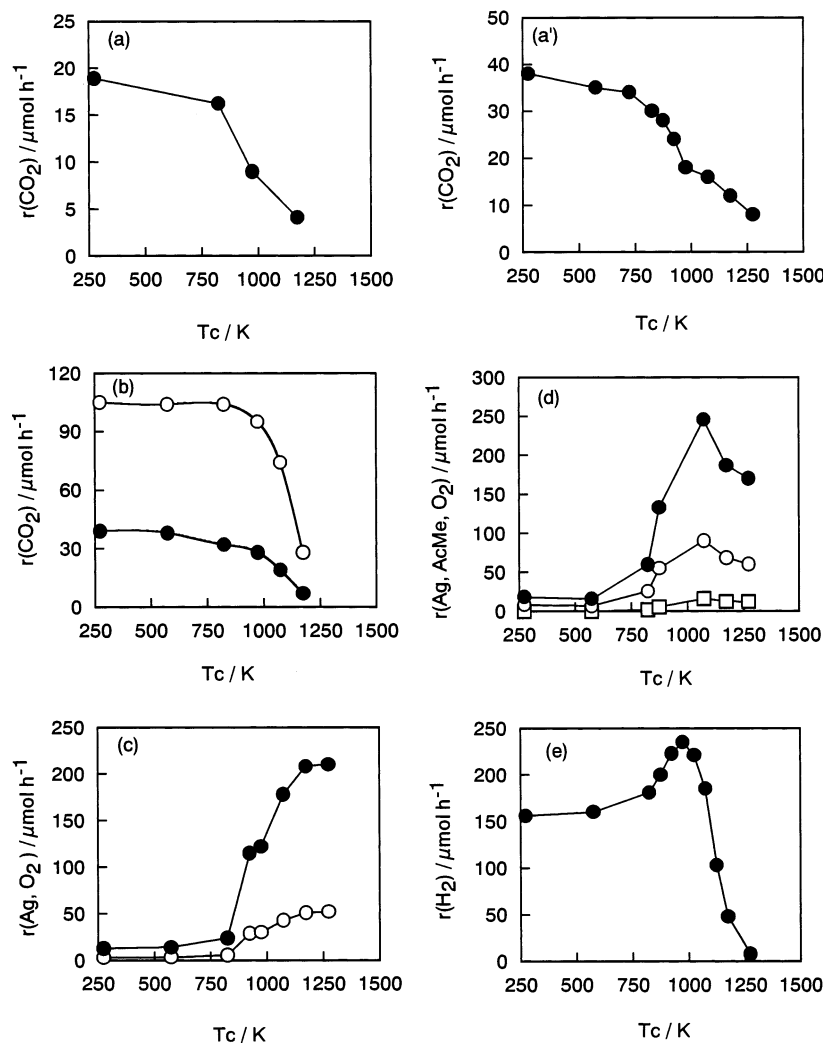


Figure 5. Dependence of the calcination temperature (T_c) on the rate of photocatalytic reactions: AcOH mineralization by (a) HyCOM-B and (a') HyCOM-A; (b) mineralization and photo-Kolbe reactions of AcOH by HyCOM-A–Pt under aerated (○) and deaerated conditions (●), respectively; (c) Ag deposition (●) along with O₂ liberation (○) by HyCOM-A; (d) Ag deposition (●) along with acetone formation (○) and O₂ liberation (□) by HyCOM-A; (e) 2-ProOH dehydrogenation by HyCOM-A–Pt.

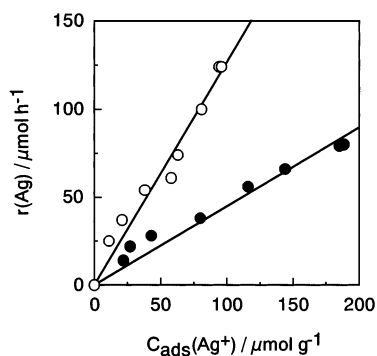


Figure 6. Rate of photocatalytic Ag deposition ($r(\text{Ag})$) as functions of the amounts of adsorbed Ag⁺ ($C_{\text{ads}}(\text{Ag}^+)$) on HyCOM-A(973) (○) and P-25 (●) in the dark.

obtained, the characteristics of Ag⁺ adsorption sites on TiO₂ are independent of the crystallite size and surface area, that is, the adsorption characteristics are not changed by calcination. If the properties of crystal bulk, for example, rate of e⁻-h⁺ recombination, are not influenced by calcination, a decrease in the photocatalytic reaction rate due to calcination is expected from the above-described behavior of $C_{\text{ads}}(\text{Ag}^+)$. However, on the other hand, the apparent rate of photocatalytic Ag deposition

was enhanced by calcination at a higher temperature as shown in Figure 5c. Similar results for this reaction have been observed in commercial TiO₂ samples⁴² and TiO₂ samples prepared by hydrolysis of titanium isopropoxide,³³ although the rate was decreased by severe calcination at 973–1173 K because of a drastic decrease in their BET surface areas.

The effect of calcination on the recombination rate for HyCOM-A was also examined by femtosecond pump-probe diffuse reflectance measurements, and it has been shown that the recombination rate was drastically decreased upon calcination.⁶³ Calcination improves crystallinity and reduces crystal defects, which predominantly act as a recombination center for e⁻-h⁺, leading to a smaller probability of recombination and enhanced photocatalytic activity. Because, as reported previously,⁵⁶ the quantum efficiency of the photocatalytic reaction by HyCOM was estimated to be ca. 30% and, thereby, a large part of e⁻-h⁺ undergoes mutual recombination, such effect of calcination diminishing the recombination seems to be reasonable. Therefore, reduced probability of e⁻-h⁺ recombination due to annealing of crystallites accounts for the increase in the photocatalytic reaction rate.

Dehydrogenation of a 2-Propanol Reaction System. Photoirradiation of the suspension of Pt-TiO₂ particles in an aqueous 2-ProOH solution under deaerated conditions leads to

almost equimolar production of acetone and H₂, as reported previously.^{33,56} The stoichiometry is represented as follows:



We could estimate the overall rate of eq 4 by measuring the initial rate of H₂ production. For all of the catalysts in this study, almost linear production of H₂ was observed in the time-course curve unless the consumption of 2-PrOH was not so marked.

Figure 5e shows the effect of T_c on the initial rate of H₂ production ($r(\text{H}_2)$) by Pt-HyCOM-A (0.1 wt %). $r(\text{H}_2)$ increased with increase in T_c until the maximum values were attained at T_c of 973 K, decreased at $T_c > 1073$ K, and became negligible at T_c of 1273 K. Similar results for this reaction were observed in TiO₂ samples prepared by hydrolysis of titanium isopropoxide (though the rate of H₂ production was decreased upon calcination at 823 K because of a decrease in the surface area).³³ This T_c dependence seemed different from those of the AcOH mineralization (Figure 5a for HyCOM-B and Figure 5a' for HyCOM-A) and the Ag deposition (Figure 5c).

We tried to measure $C_{\text{ads}}(2\text{-PrOH})$ by several analytical procedures but failed mainly because of the relatively high detection limits compared with the adsorption amount when measured under the conditions similar to the photocatalytic reaction. According to the dependence of $C_{\text{ads}}(\text{AcOH})$ and $C_{\text{ads}}(\text{Ag}^+)$ on T_c of the HyCOM powders, we can expect a constant surface density of 2-PrOH on the TiO₂ surface, that is, that $C_{\text{ads}}(2\text{-PrOH})$ is almost proportional to the specific surface area of each TiO₂. Assuming this, we can attribute the enhancement of photocatalytic activity at T_c between 750 and 1100 K to a decrease in the $e^- - h^+$ recombination rate as observed in the Ag deposition system. The crystal transformation from anatase into rutile might affect the activity at $T_c > 1073$ K, but at least at a relatively low T_c , the increase in $r(\text{H}_2)$ is accounted by the growth of anatase crystallite, that is, reduction of crystal defects working as a recombination center. Furthermore, the possibility of a probable different mode of Pt loading could be excluded because the same Pt-HyCOM-A showed a T_c dependence of $r(\text{CO}_2)$, which did not give a peak in the activity and was similar to that for bare HyCOM-A at $T_c < 973$ K. Thus, it has been proved that in this 2-PrOH dehydrogenation system both adsorbability and recombination factors are required for high activity.

T_c Dependence of Photocatalytic Activity. As depicted in Figure 5, an appreciable difference in the photocatalytic activity depending on T_c was seen for several kinds of reaction systems. Except for the case of 2-PrOH dehydrogenation, it has been proved that the activity of each TiO₂ sample is almost proportional to the amount of the reaction substrate, that is, AcOH and Ag⁺ in the AcOH mineralization and Ag deposition systems, respectively. Taking these facts into consideration, a possible reason for the different T_c dependencies is that the TiO₂ samples have different distributions of active and inactive phases, both of which adsorb the reaction substrate. For example, it can be assumed that anatase and amorphous phases are mixed in different ratios depending on T_c and that both phases adsorb the substrate with almost the same equilibrium constant, K_{ads} . If, for the Ag deposition, only anatase crystallites show photocatalytic activity, the enhanced activity with increase in T_c can be explained by the increasing content of the active anatase phase, that is, the increasing amount of adsorbed Ag⁺ on the anatase surface. On the other hand, for the AcOH mineralization, both anatase and amorphous phases are sufficiently active to result in the photocatalytic activity being proportional to the specific surface area of each TiO₂ sample.

At present, it is difficult to estimate the ratios of active and inactive phases in the samples. Furthermore, we cannot discriminate the rate of photocatalytic reaction and the amount of substrates on amorphous and anatase phases in their mixture, though the photocatalytic activities of anatase and rutile phases in their mixture have been separately estimated by using their different photoabsorption characteristics.⁶⁶ The important point is to clarify the low or negligible photocatalytic activity of the inactive, presumably a kind of amorphous, phase. On the basis of previous results for pure amorphous samples, it is thought that the recombination of $e^- - h^+$ occurs more quickly in the amorphous phase than in the other crystalline phase. Therefore, the inactive phase should be, in other words, the defective part of samples of a higher recombination rate. Our working hypothesis is that the number of electrons (or holes) required to complete the photocatalytic reactions determines the T_c dependence, that is, the larger the number becomes, the more the recombination probability is affected. For mineralization of AcOH, the number is presumed to be one; one-electron (hole) oxidation of AcOH adsorbed on the TiO₂ surface can be a significant process to determine the overall rate, because a proposed intermediate radical undergoes feasible addition of O₂ followed by thermal degradation.⁶⁷ In this reaction system, e^- and h^+ do not need to migrate in the TiO₂ particle before completing the reaction, that is, the adsorbability becomes a more significant factor determining the photocatalytic activity than does the recombination property. The dehydrogenation of 2-PrOH is formally a two-electron process. Being different from these reactions, completion of Ag deposition together with O₂ evolution requires four electrons. In other words, four holes must migrate in the particle, escaping from the recombination, before arriving at the site for O₂ evolution. It seems that, under these circumstances, the recombination probability becomes a more significant factor determining the photocatalytic activity. TiO₂ powders prepared and calcined at low temperature adsorb large amounts of substrates but contain a large number of crystal defects, and migration of active species may therefore be markedly suppressed. On the other hand, HyCOM-A and HyCOM-B calcined at higher T_c exhibited superior photocatalytic activity, especially when the reaction required many electrons (holes).

Consistent with the above arguments, we could see an improvement in photocatalytic activity of HyCOM-A calcined at a temperature between 823 and 1073 K by adding 2-PrOH (0.5 mmol) to the starting Ag₂SO₄ solution (Figure 5d); for example, the rates for Ag deposition (together with acetone formation, $2\text{Ag}^+ + \text{CH}_3\text{CHOHCH}_3 = 2\text{Ag} + \text{CH}_3\text{COCH}_3 + 2\text{H}^+$)^{33,50} by HyCOM-A(823) and HyCOM-A(1073) were increased from 25 and 149 to 60 and 245 $\mu\text{mol h}^{-1}$, respectively. Essentially the same behavior has been reported earlier for TiO₂ powders prepared from alkoxide.³³ This may be accounted for by the change in the number of electrons from 4 (O₂) to 2 (acetone). At higher T_c , the rate of Ag deposition was not greatly improved because, in such a high T_c region, the surface area of samples was reduced to affect the overall activity as seen in the 2-PrOH dehydrogenation system.

IV. Conclusions

The physical properties of HyCOM TiO₂ powders, for example, surface area, particle size, and adsorbability of substrates, can be controlled over a wide range by changing the postcalcination temperature (T_c) up to 1273 K. The effects of calcination on the photocatalytic activities for several photocatalytic reactions were studied, and it was found that the

activities strongly depend on the extents of two significant physical factors for active photocatalysts: adsorbability and recombination probability. Their difference in the T_c dependence could be interpreted reasonably by the number of electrons (or holes) required to complete the photocatalytic reaction; the larger the number becomes, the more the recombination probability affects the reaction rate. Thus, we have shown correlations of the physical properties of TiO₂ powders with photocatalytic activities in diverse photocatalytic reaction systems. These results provide important information for the design and synthesis of highly active semiconductor photocatalysts by taking the reaction types into consideration.

Acknowledgment. This work was partly supported by grants-in-aid from the Ministry of Education, Science, Sports, and Culture of Japan (Grants 09750861, 09218202, and 09044114 and Priority Areas 417). One of the authors (S.-y.M.) is grateful for the Sasagawa Scientific Research Grant from The Japan Science Society.

References and Notes

- (1) Fujishima, A.; Honda, K. *Nature (London)* **1972**, *37*, 238.
- (2) Sato, S.; White, J. M. *Chem. Phys. Lett.* **1980**, *72*, 83.
- (3) Kudo, A.; Domen, K.; Maruya, K.; Onishi, T. *Chem. Phys. Lett.* **1987**, *133*, 517.
- (4) Tabata, S.; Nishida, H.; Masaki, Y.; Tabata, K. *Catal. Lett.* **1995**, *34*, 245.
- (5) Sayama, K.; Arakawa, H. *J. Chem. Soc., Faraday Trans.* **1997**, *93*, 1647.
- (6) Kudo, A. *Hyomen* **1998**, *36*, 625.
- (7) Moon, S.-C.; Mametsuka, H.; Suzuki, E.; Nakahara, Y. *Catal. Today* **1998**, *45*, 79.
- (8) Kominami, H.; Murakami, S.-y.; Kohno, M.; Kera, Y.; Okada, K.; Ohtani, B. *Phys. Chem. Chem. Phys.* **2001**, *3*, 4102.
- (9) Kawai, T.; Sakata, T. *Nature (London)* **1980**, *286*, 474.
- (10) Pichat, P.; Herrmann, J. M.; Disdier, J.; Courbon, H.; Mozzanega, M. N. *Nouv. J. Chim.* **1981**, *5*, 627.
- (11) Teratani, S.; Nakamichi, J.; Taya, K.; Tanaka, K. *Bull. Chem. Soc. Jap.* **1982**, *55*, 1688.
- (12) Domen, K.; Naito, S.; Onishi, T.; Tamaru, K. *Chem. Lett.* **1982**, 555.
- (13) Nishimoto, S.-i.; Ohtani, B.; Kagiya, T. *J. Chem. Soc., Faraday Trans. 1* **1985**, *81*, 2467.
- (14) *Photocatalytic Purification and Treatment of water and Air*; Ollis, D. F., Al-Ekabi, H., Eds.; Elsevier: Amsterdam, 1993.
- (15) Kamat, P. V. *Chem. Rev.* **1993**, *93*, 267.
- (16) Hoffmann, M. R.; Martin, S. T.; Choi, W.; Bahnemann, D. W. *Chem. Rev.* **1995**, *95*, 69.
- (17) Loddo, V.; Marci, G.; Martin, C.; Palmisano, L.; Rives, V.; Sclafani, A. *Appl. Catal. B* **1999**, *20*, 29.
- (18) Nishimoto, S.-i.; Ohtani, B.; Yoshikawa, T.; Kagiya, T. *J. Am. Chem. Soc.* **1983**, *105*, 7180.
- (19) Fox, M. A.; Dulay, M. T. *Chem. Rev.* **1993**, *93*, 341.
- (20) Mahdavi, F.; Bruton, T. C.; Li, Y. *J. Org. Chem.* **1993**, *58*, 744.
- (21) Jia, J.; Ohno, T.; Masaki, Y.; Matsumura, M. *Chem. Lett.* **1999**, 963.
- (22) Ohtani, B.; Kusakabe, S.; Okada, K.; Tsuru, S.; Nishimoto, S.-i.; Amino, Y.; Izawa, K.; Nakato, Y.; Matsumura, M.; Nakaoka, Y.; Nosaka, Y. *J. Chem. Soc., Perkin Trans. 2* **2001**, 201.
- (23) Inoue, T.; Fujishima, A.; Konishi, S.; Honda, H. *Nature* **1979**, *277*, 633.
- (24) Henglein, A.; Gutierrez, M.; Fisher, C.-H. *Ber. Bunsen-Ges. Phys. Chem.* **1984**, *88*, 170.
- (25) Cook, R. L.; MacDuff, R. C.; Sammells, A. F. *J. Electrochem. Soc.* **1988**, *135*, 3069.
- (26) Irvine, J. T. *Sol. Energy* **1990**, *45*, 27.
- (27) Inoue, H.; Kudo, Y.; Yoneyama, H. *J. Chem. Soc., Faraday Trans.* **1991**, *87*, 553.
- (28) Ishitani, O.; Inoue, T.; Suzuki, K.; Ibusuki, T. *J. Photochem. Photobiol., A: Chem.* **1993**, *72*, 269.
- (29) Fujiwara, H.; Hosokawa, H.; Murakoshi, K.; Wada, Y.; Yanagida, S.; Okada, T.; Kobayashi, H. *J. Phys. Chem. B* **1997**, *101*, 8270.
- (30) *Photocatalysis: Fundamentals and Applications*; Sepone, N., Pelizzetti, E., Eds.; John Wiley & Sons: New York, 1989.
- (31) *Heterogeneous Photocatalysis*; Schiavello, M., Ed.; John Wiley & Sons: New York, 1997.
- (32) Mills, A.; Porter, G. *J. Chem. Soc., Faraday Trans. 1* **1982**, *78*, 3659.
- (33) Nishimoto, S.-i.; Ohtani, B.; Kajiwara, H.; Kagiya, T. *J. Chem. Soc., Faraday Trans. 1* **1985**, *81*, 61.
- (34) Bickley, R. I.; Gonzalez-Carreno, T.; Lees, J. S.; Palmisano, L.; Tilley, R. J. D. *J. Solid State Chem.* **1991**, *92*, 178.
- (35) Sakata, T.; Kawai, T.; Hashimoto, K. *Chem. Phys. Lett.* **1982**, *88*, 50.
- (36) Ohtani, B.; Hanada, J.-i.; Nishimoto, S.-i.; Kagiya, T. *Chem. Phys. Lett.* **1985**, *120*, 292.
- (37) Sclafani, A.; Palmisano, L.; Schiavello, M. *J. Phys. Chem.* **1990**, *94*, 829.
- (38) Tanaka, K.; Capule, M. F. V.; Hisanaga, T. *Chem. Phys. Lett.* **1991**, *187*, 73.
- (39) Ohtani, B.; Zhang, S.-W.; Nishimoto, S.-i.; Kagiya, T. *J. Photochem. Photobiol., A: Chem.* **1992**, *64*, 223.
- (40) Oosawa, Y.; Gratzel, M. *J. Chem. Soc., Chem. Commun.* **1984**, 1629.
- (41) Ohtani, B.; Okugawa, Y.; Nishimoto, S.-i.; Kagiya, T. *J. Phys. Chem.* **1987**, *91*, 3350.
- (42) Oosawa, Y.; Gratzel, M. *J. Chem. Soc., Faraday Trans. 1* **1988**, *84*, 197.
- (43) Nishiwaki, K.; Kakuta, N.; Ueno, A.; Nakabayashi, H. *J. Catal.* **1989**, *118*, 498.
- (44) Montoya, I. A.; Viveros, T.; Dominguez, J. M.; Canales, L. A.; Shifter, I. *Catal. Lett.* **1992**, *15*, 207.
- (45) Barringer, E. A.; Bowen, H. K. *J. Am. Ceram. Soc.* **1982**, *65*, 199.
- (46) Oguri, Y.; Riman, R. E.; Bowen, H. K. *J. Mater. Sci.* **1988**, *23*, 2397.
- (47) Kondo, M.; Shinozaki, K.; Ooki, R.; Mizutani, N. *J. Ceram. Soc. Jpn.* **1994**, *102*, 742.
- (48) Nishimoto, S.-i.; Ohtani, B.; Kajiwara, H.; Kagiya, T. *J. Chem. Soc., Faraday Trans. 1* **1983**, *79*, 2685.
- (49) Ohtani, B.; Kakimoto, M.; Nishimoto, S.-i.; Kagiya, T. *J. Phys. Chem.* **1988**, *92*, 5773.
- (50) Ohtani, B.; Nishimoto, S.-i. *J. Phys. Chem.* **1993**, *97*, 920.
- (51) Ohtani, B.; Tennou, K.; Nishimoto, S.-i.; Inui, T. *J. Photosci.* **1995**, *2*, 7.
- (52) Ohtani, B.; Iwai, K.; Nishimoto, S.-i.; Sato, S. *J. Phys. Chem. B* **1997**, *101*, 3349.
- (53) Ohtani, B.; Ogawa, Y.; Nishimoto, S.-i. *J. Phys. Chem. B* **1997**, *101*, 3746.
- (54) Kominami, H.; Takada, Y.; Yamagiwa, H.; Kera, Y.; Inoue, M.; Inui, T. *J. Mater. Sci. Lett.* **1996**, *15*, 197.
- (55) Kominami, H.; Kohno, M.; Takada, Y.; Inoue, M.; Inui, T.; Kera, Y. *Ind. Eng. Chem. Res.* **1999**, *38*, 3925.
- (56) Kominami, H.; Matsuura, T.; Iwai, K.; Ohtani, B.; Nishimoto, S.-i.; Kera, Y. *Chem. Lett.* **1995**, 693.
- (57) Kominami, H.; Murakami, S.-y.; Kera, Y.; Ohtani, B. *Catal. Lett.* **1998**, *56*, 125.
- (58) Ohtani, B.; Iwai, K.; Kominami, H.; Matsuura, T.; Kera, Y.; Nishimoto, S.-i. *Chem. Phys. Lett.* **1995**, *242*, 315.
- (59) Kominami, H.; Kato, J.-i.; Kohno, M.; Kera, Y.; Ohtani, B. *Chem. Lett.* **1996**, 1051.
- (60) Kominami, H.; Kato, J.-i.; Takada, Y.; Doushi, Y.; Ohtani, B.; Nishimoto, S.-i.; Inoue, M.; Inui, T.; Kera, Y. *Catal. Lett.* **1997**, *46*, 235.
- (61) Kominami, H.; Kato, J.-i.; Murakami, S.-y.; Kera, Y.; Inoue, M.; Inui, T.; Ohtani, B. *J. Mol. Catal. A* **1999**, *144*, 165.
- (62) Bickley, R. I.; Stone, F. S. *J. Catal.* **1973**, *31*, 389.
- (63) Ohtani, B.; Bowman, R. M.; Colombo, D. P., Jr.; Kominami, H.; Noguchi, H.; Uosaki, K. *Chem. Lett.* **1998**, 579.
- (64) Fleischauer, P. D.; Kan, H. K. A.; Shepherd, J. R. *J. Am. Chem. Soc.* **1972**, *94*, 283.
- (65) Martin, S. T.; Herrmann, H.; Choi, W.; Hoffmann, M. R. *J. Chem. Soc., Faraday Trans.* **1994**, *90*, 3315.
- (66) Torimoto, T.; Nakamura, N.; Ikeda, S.; Ohtani, B., to be submitted for publication.
- (67) Kato, K.; Tsuzuki, A.; Torii, Y.; Taoda, H.; Kato, T.; Butsugan, Y. *J. Mater. Sci.* **1995**, *30*, 837.